Application of electrochemical treatment for the removal of triazine dye using aluminium electrodes

Sakthisharmila Palanisamy, Palanisamy Nachimuthu, Mukesh Kumar Awasthi, Balasubramani Ravindran, Soon Woong Chang, Manikandan Palanichamy and Dinh Duc Nguyen

ABSTRACT

Textile effluents contain triazine-substituted reactive dyes that cause health problems such as cancer, birth defects, and hormone damage. An electrochemical process was employed effectively to degrade azo reactive dye with the aim of reducing the production of carcinogenic chemicals during biodegradation. Textile dye C.I. Reactive Red 2 (RR2), a model pollutant that contains dichloro triazine ring, was subjected to the electrocoagulation process using aluminium (Al) electrodes. A maximum of 97% of colour and 72% of chemical oxygen demand (COD) removal efficiencies were achieved and 9.5 kWh/kg dye electrical energy and 0.8 kg Al/kg dye electrode consumption were observed. The dye removal mechanism was studied by analysing the results of UV-Vis spectra of RR2 and treated samples at various time intervals during electrocoagulation. Fourier transform infrared (FTIR) spectra and energy dispersive X-ray (EDX) spectral studies were used for analysing the electrocoagulated flocs. The results indicate that in this process the dye gets removed by adsorption and there is no significant carcinogenic by-product formation during the degradation of dye.

Key words | chemical oxygen demand, degradation, electrochemical process, textile dye, textile effluent

Sakthisharmila Palanisamy
Department of Chemistry,
Bannari Amman Institute of Technology,
Sathyamangalam 638 401,
India

Palanisamy Nachimuthu
Manikandan Palanichamy
Centre for Environmental Research, Department of Chemistry,
Kongu Engineering College,
Perundurai 638060,
India

Mukesh Kumar Awasthi
College of Natural Resources and Environment,
Northwest A&F University,
Yangling, Shaanxi Province 712100,
China

Balasubramani Ravindran
Soon Woong Chang
Dinh Duc Nguyen (corresponding author)
Department of Environmental Energy Engineering,
Kyonggi University,
Youngtong – Gu, Suwon 16227,
Korea
E-mail: *kalamravi@gmail.com*

Dinh Duc Nguyen
Faculty of Environmental and Food Engineering,
Nguyen Tat Thanh University,
300A Nguyen Tat Thanh, District 4, Ho Chi Minh City, 755414,
Vietnam

INTRODUCTION

Textile industries use different types of fabrics for dyeing and produce large quantities of wastewater. Approximately 1,000–3,000 m^3 of wastewater is produced for every 10,886.2–18,143.7 kg of textile fabrics processed (Al-Kdasi *et al.* 2004). Textile wastewater consists of unfixed dyes, inorganic and organic chemicals and trace metals that are harmful to the environment and can cause haemorrhage, nausea, skin diseases, cancer, and mutagenesis (Ghaly *et al.* 2014). Textile wastewater is characterised by high colour content due to the presence of unfixed dyes, which affects its biodegradability by reducing the penetration of light and decreases the dissolved oxygen content (Muthukumar *et al.* 2007). The fixation of dyes on fabrics depends on the nature of the dyes and fabrics. To increase fixation, heterofunctional dyes such as sulfonic and chlorine substituted triazine groups containing azo dyes are used in industries; however, dyes containing chloro-substituted triazines are easily

doi: 10.2166/aqua.2020.109

hydrolysed and get converted into their constituent components (Sala *et al.* 2014). Hence, the removal of these dyes is difficult, and only limited methods can be adopted for the removal of triazine-substituted dyes from textile industrial effluents.

The abatement of RR2 triazine dye from wastewater is carried out using various adsorbents such as *Metapenaeus monoceros* shell (Thiyagarajan *et al.* 2013), nanoscale zerovalent iron (Lin & Chen 2017), Fe_3O_4 nanoparticles (Lin *et al.* 2016) and textile sludge (Sonai *et al.* 2016). Catalysts such as anthraquinone-2,6-disulfonate (AQDS) (Costa *et al.* 2010) and platinised titanium dioxide (Kuo & Lin 2009) are used to remove RR2 from aqueous solution. Catalytic ozonation, iron powder reduction and photooxidation (Feng *et al.* 2000), biodegradation using *Pseudomonas sp. SUK1*, advanced oxidation (Wu & Ng 2008) and UV/chlorine advanced oxidation (Wu *et al.* 2016) have been employed for treating RR2 contained wastewater.

The current study focuses on the use of electrochemical methods for the removal of textile dyes from wastewater. Electrochemical methods are classified with respect to the electrode material, used chemicals and the pollutant removal mechanism. Well known electrochemical methods are electro-oxidation (using stable electrodes such as PbO_2, mixed metal oxides (MMO) and RuO_2), electro-Fenton, and peroxi-coagulation (using H_2O_2 as an activator). Electrocoagulation is cost-effective, operationally simple, with no sensitivity to toxicity and has less sludge generation than other processes (Nguyen *et al.* 2014b, 2016). The theory of the process is described as the generation of metal ions from anodes hydrolysed into metal hydroxides, and the generation of hydrogen (H_2) bubbles that occur at the cathode which help the coagulated matters to float (Equations (1)–(4)) (Mollah *et al.* 2004; Ozyonar & Karagozoglu 2011). The performance of the electrocoagulation process depends on wastewater properties, especially pH, conductivity, and chemical composition. The electrocoagulation process involves three successive stages for pollutant removal: (i) generation of coagulants by the oxidation of electrodes in an electrolyte solution, (ii) destabilisation of pollutants and suspensions by compression of diffuse double layer and charge neutralisation and (iii) agglomeration of destabilised pollutants with coagulants (Singh *et al.* 2014). The electrocoagulation process is applied for the removal of some triazine substituted azo dyes, such as reactive yellow 84 and reactive blue 49 which are removed using Al, Fe and stainless steel (SS) electrodes. Reactive orange 84 is eliminated using Fe and SS electrodes (Kim *et al.* 2002; Yuksel *et al.* 2013). A central composite design (CCD) modelling software is utilised to optimise the removal of reactive red 141 (Salmani *et al.* 2016) with Fe electrodes and reactive red 198 (Khosravi *et al.* 2015) with Al electrodes. He *et al.* (2007) experimented with the decolourisation of reactive yellow 84 by electrocoagulation which is enhanced with ozonation. The degradation of reactive red 120 is studied by using the electrocoagulation process and the dye degradation mechanism is analysed through gas chromatography mass spectrometry (GC-MS) studies (Pirkarami & Olya 2014).

At anode:

$$Al \rightarrow Al^{3+} + 3e^- \tag{1}$$

At cathode:

$$3H_2O + 3e^- \rightarrow \frac{3}{2}H_{2(g)} + 3OH^- \tag{2}$$

In the solution;

$$Al^{3+} + 3H_2O \rightarrow Al(OH)_3 + 3H^+_{(Aq)} \tag{3}$$

$$nAl(OH)_3 \rightarrow Al_n(OH)_{3n} \tag{4}$$

Based on the reported literature, the removal of RR2 dye was studied by varying key process parameters of the electrocoagulation process such as: solution pH (3–11), applied potential (2–6 V), electrolyte (NaCl) concentration (1–3 g/L), dye solution concentration (100–500 ppm), active surface area of electrodes (10–30 cm^2) and inter-electrode distance (2–4 cm). The process efficiency was optimised based on parameters of colour, chemical oxygen demand (COD) removal efficiencies, electrical energy and electrode consumption, and operational cost. The dye abatement mechanism during the treatment was analysed with UV-visible, Fourier transform infrared (FTIR) spectra and energy dispersive X-ray (EDX) spectral studies.

MATERIALS AND METHODS

C.I reactive red 2 (RR 2) ($C_{19}H_{10}Cl_2N_6Na_2O_7S_2$, MW 615.34 g/mol) was selected as a typical model pollutant, and the molecular structure of dye is depicted in Figure S1 (Supplementary Data). The textile dye was dissolved in distilled water and stored as a stock solution (5,000 ppm). Before the experiment, a certain concentration of dye solution was prepared by diluting the stock solution. The solution pH and conductivity were adjusted using dilute HCl (0.1 N), NaOH (0.1 N) and NaCl (1–3 g/L). Variations in pH (ELICO pH LI 120) and conductivity (CM 180) were measured using respective meters. A working volume of 0.3 L was placed in the reactor and an Al (HE18) electrode (dimensions $15 \times 15 \times 0.1$ cm) was fitted in the reactor with the help of non-conducting holders which maintained the desired effective surface area of the electrode. During the experiment, the residual dye concentration was measured using a UV-Vis Spectrometer (DR3900, Hach Company, USA) and the UV-Vis spectra were recorded with an ELICO (BL198) spectrophotometer. The dye solution was collected at different time intervals. It was filtered using Whatman filter paper (size 41), and the COD was measured as per the standard protocol (APHA/AWWA/WEF 2005). After electrocoagulation, electrocoagulated flocs were collected, filtered, and dried at 105 °C in a hot air oven. Dried flocs were subjected to FTIR analysis which was carried out using a JASCO (FT-IR-V 400 series) spectrophotometer.

The COD removal efficiency based on colour change was calculated by the following equation:

$$Y = \frac{(C_0 - C_t) \cdot 100}{C_0} \tag{5}$$

where Y is the colour or COD removal efficiency, C_0 is the initial concentration of RR2 or COD (ppm) and C_t is the concentration of RR2 or COD (ppm) at time t (min).

The electrical energy (kWh/kg of dye) and electrode consumption (kg of Al/kg of dye) are calculated as represented in Equations (6) and (7) (Şengil & Özacar 2009):

$$Electrical\ energy\ consumption = \frac{V \cdot I \cdot t \cdot 10^3}{60 \cdot (C_0 - C_t) \cdot v} \tag{6}$$

$$Electrode\ consumption = \frac{M \cdot I \cdot t}{n \cdot F \cdot v \cdot (C_0 - C_t)} \tag{7}$$

where V is the applied potential (V), I is an applied current (A), t is the time of electrolysis (min), and v is the working volume of dye solution (L). M is the molecular mass of Al (g Mol^{-1}), n is the number of electrons contributed in the reaction (Al = 3), and F is the Faraday constant (F = 96,487 C Mol^{-1}).

The current efficiency of the electrocoagulation process is the calculated ratio between actual release of aluminium ions and theoretical value as shown below (Ahmadi & Ghanbari 2016):

$$CE = \frac{m_a}{\frac{ItM}{nF}} \times 100 \tag{8}$$

where CE is current efficiency, m_a is the actual mass of Al ions released as calculated by the weight loss of electrodes before and after treatment.

The rate of dye removal efficiency of Al electrodes can be represented by the pseudo first-order reaction:

$$Ln\left(\frac{C_0}{C_t}\right) = k \cdot t \tag{9}$$

where k is the pseudo first-order rate constant (min^{-1}). Equation (9) indicates that a plot of Ln (C_0/C_t) against t would be a straight line with a slope of k (El-Ashtoukhy & Amin 2010).

Similarly, the voltage drop (h_{IR}) is governed by the following equation (Ghosh *et al.* 2008):

$$h_{IR} = \frac{I \cdot d}{A \cdot k} \tag{10}$$

where d is the inter-electrode distance of two electrodes (m) in an electrocoagulation reactor, A is the active surface area

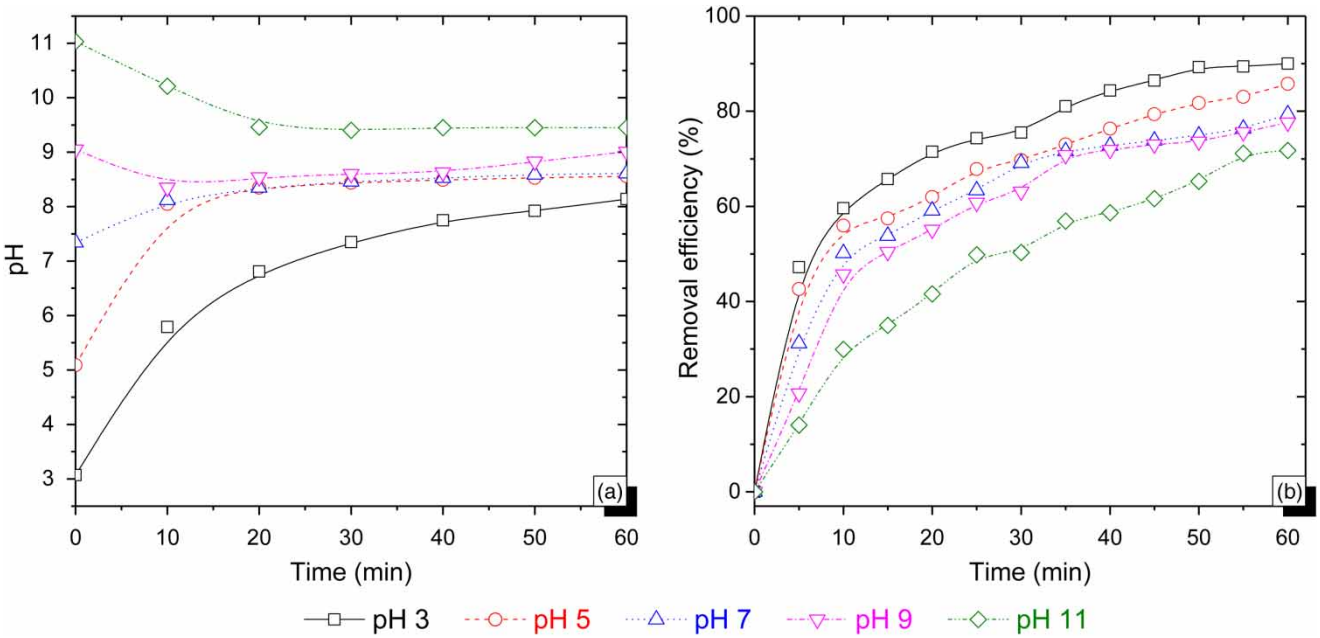

Figure 1 | Effect of solution pH: (a) change of solution pH and (b) colour removal efficiency with respect to time.

of the anode (m^2), and k is the electrical conductivity of the dye solution (mS/m).

RESULTS AND DISCUSSION

Effect of solution pH in the removal of RR2

During the electrocoagulation process, solution pH variations and colour removal efficiency were studied and the results are depicted in Figure 1(a) and 1(b). During the electrolysis, dye removed water pH was raised to alkaline medium while the initial pH of dye solution is fixed at 3, 5 and 7. The increase in pH after the treatment is due to the generation of hydroxyl ions which is generated from the cathodic site during the electrolysis of dye solution. The dye solution pH is fixed at 9 and it is maintained throughout the process. The dye solution pH is increased to 11 before the treatment and it is decreased to 9.5 after the treatment. The initial pH 9 and 11 are buffered to pH 9 because the generated hydroxyl ions are equilibrated with aluminium ions, which is caused by the chemical dissolution of aluminium electrodes at basic medium (Amour *et al.* 2016; Nguyen *et al.* 2017). The change in solution pH before the experiment affected the performance of Al electrodes and this is evidenced by colour removal efficiency which is decreased by 89.98, 79.83 and 71.73% whereas the initial pH of dye solution is fixed at 3, 7 and 11, respectively. Figure 1(b) shows that when the electrocoagulation time increases, the colour removal efficiency increases in all ranges of pH up to 45 min and then reaches equilibrium. This behaviour is caused by the different mechanisms followed by the dye removal process, such as precipitation, charge neutralisation, and adsorption (Barrera-Díaz *et al.* 2012), as shown in Equations (11)–(14).

$$\left.\begin{array}{l} Dye + monomeric\ Al \rightarrow [Dye\ monmerical\ Al]_s \quad (11) \\ Dye + polymeric\ Al \rightarrow [Dye\ polymerical\ Al]_s \quad (12) \end{array}\right\rangle$$

Precipitation

$$\left.\begin{array}{l} Dye + Al\ (OH)_{3(s)} \rightarrow [Particle] \quad (13) \\ [Dye\ polymerical\ Al] + Al\ (OH)_{3(s)} \rightarrow [Particle] \quad (14) \end{array}\right\rangle$$

Adsorption

The highest enhanced colour removal efficiency was achieved at pH 3 due to the combined effect of these

mechanisms with the increase of solution pH with time. The lower colour removal efficiency was observed at alkaline (pH 9 and 11), which may be caused by the repulsion between anionic dye molecules and Al $(OH)_4^-$ ions.

Effect of an applied potential in the removal of RR2

The generation of metal hydroxide flocs and bubble formation is amplified with the increase in applied voltage. The colour removal effectiveness increased from 60.07 to 79.38% whereas the applied potential varied from 2 to 4 V. When further increasing the applied potential from 5 to 6 V, the colour removal efficiency slightly increased (Figure 2). According to Faraday's law, the metal dissolution and floc generations are directly proportional to the current density of the reactor (Daneshvar *et al.* 2007). The metal hydroxide increases with the increase in applied voltage, which is attributed to colour removal efficiency up to 4 V. The colour removal efficiency attained at 5 and 6 V is due to unsaturated concentration dye and metal hydroxides. The COD removal efficiency was improved from 25.37 to 65.07% by raising the applied potential from 2 to 6 V. The energy consumption was calculated as 0.71 and 12.05 kWh/kg for applied potentials of 2 and 6 V, respectively. The final pH of the treated solution is approximately 8.5, which shows that the applied potential does not affect the reaction scheme.

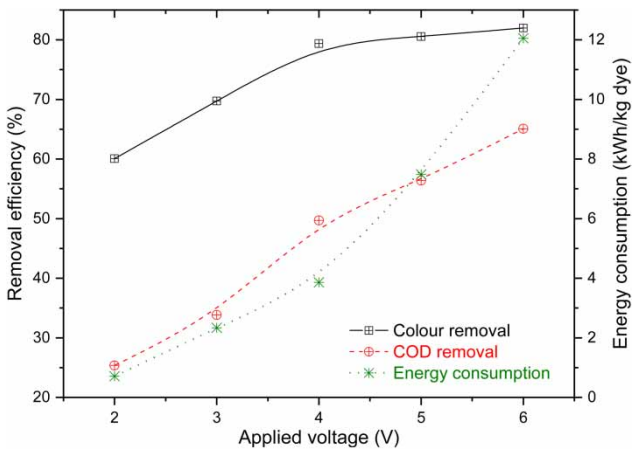

Figure 2 | Effect of an applied potential in the removal of RR2.

Effect of an electrolyte dosage in the removal of RR2

The addition of electrolytes leads to an increase in the conductivity of the dye solution which reduces the ohmic resistance among the electrodes (Nguyen *et al.* 2014a; Nandi & Patel 2017). The electrolyte concentration increases the current density of electrocoagulation reactor at the same applied voltage (Şengil & Özacar 2009). In major studies, NaCl is selected as an electrolyte to perform electrocoagulation as it is used for dye fixation in textile industries. It also acts as a pitting agent to remove oxide films from the electrode's surface (Pajootan *et al.* 2012; Pirkarami & Olya 2014). In this study, the conductivity of the dye solution ranges from 3.36 to 8.24 mS/cm for NaCl dosages of 1–3 g/L, respectively. It leads to a change in voltage drop from 2.5 to 3.07 V which simultaneously influences the increase in energy and electrode consumption from 3.86 to 10.14 kWh/kg dye and 0.32 to 0.85 kg Al/kg dye. The high concentration of electrolyte leads to more metal dissolution (Mbacké *et al.* 2016) which enhances the colour removal efficiency from 79.38 to 86.93% by raising the electrolyte concentration from 1 to 3 g/L (Table 1). From the above results, it can be concluded that increasing electrolyte concentration greatly affects the energy and electrode consumption.

Effect of an initial dye concentration in the removal of RR2

Characterisation of real-time textile effluents shows fluctuating values of COD and different colour intensities (Manikandan *et al.* 2015). Concentration of RR2 varies

Table 1 | Effect of electrolyte (NaCl) concentration on colour removal efficiency, energy and electrode consumption

NaCl concentration (g/L)	Colour removal efficiency (%)	Energy consumption (kWh/kg dye)	Electrode consumption (kg Al/kg dye)	Voltage drop ($\times 10^{-3}$ V)
1	79.38	3.86	0.32	2.50
1.5	81.86	4.83	0.40	2.68
2	84.09	6.80	0.57	2.72
2.5	85.81	8.30	0.70	2.91
3	86.93	10.14	0.85	3.07

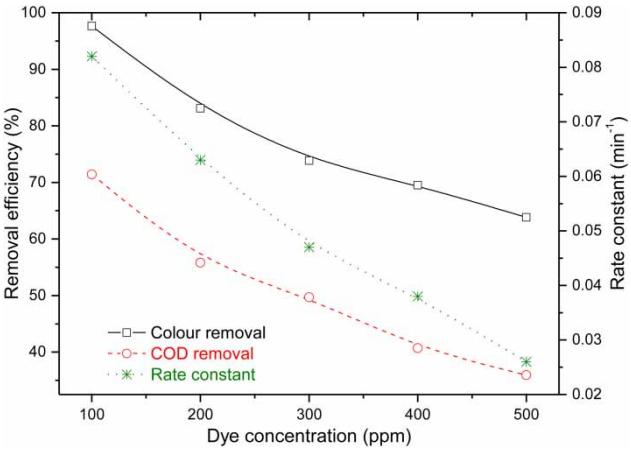

Figure 3 | Effect of an initial dye concentration in the removal of RR2.

between 100 and 500 ppm to study the colour parameters, COD abatement efficiencies, and kinetics. With an increase in the dye concentration from 100 to 500 ppm, the colour and COD removal efficiencies decrease from 97.65 to 63.89% and 71.43 to 35.92%, respectively (Figure 3). The pseudo first-order kinetics was studied to determine the rate of colour removal efficiency. This rate constant value decreases from 0.082 to 0.026 min^{-1} while the dye concentration increases from 100 to 500 ppm. The decrease in colour, COD abatement efficiencies and rate constant at different dye concentrations are due to the generation of coagulants. The coagulant generation rate is found to be constant at the same current density. The generation of an inadequate amount of coagulants at a constant current density prevents the removal of dye molecules at high concentration of dyes from aqueous solution (Nandi & Patel 2014).

Table 2 | Effect of electrode surface area on colour removal efficiency, energy consumption and amount of dye removed per unit area of electrode

Surface area of electrode (cm^2)	Colour removal efficiency (%)	Energy consumption (kWh/kg dye)	Amount of dye removed per unit area of electrode (ppm/cm^2)
10	53.24	3.18	16.77
15	62.31	3.45	12.89
20	69.14	3.76	10.63
25	79.39	3.86	9.67
30	84.10	4.18	8.50

Effect of an active surface area of electrode in the removal of RR2

The electrode active surface area in the electrocoagulation reactor varies from 10 to 30 cm^2. The colour removal efficiency, electrical energy, and electrode consumption are shown in Table 2. The colour removal efficiency increases from 53.24 to 84.10% with an increase in the electrode active surface area of 10–30 cm^2. A similar trend has been observed by Daneshvar *et al.* (2003). The colour removal efficiency due to the floc density and distribution increases with the active surface area of electrode. At certain voltages, the passage of current increases with the increase in the active surface area of the electrode which affects the electrical energy use. The highest value of electrical energy consumption was 4.18 kWh/kg when the electrode active surface area was 30 cm^2. It was observed that the dye removal capacity per unit area of electrodes decreased from 16.77 to 8.50 ppm/cm^2 when the surface area of the electrode increased from 10 to 30 cm^2 (Table 2). The increasing concentration of flocs is unsaturated with the decreasing concentration of dye during the course of the experiment (Sakthisharmila *et al.* 2017). Therefore, the dye removal capacity decreases while increasing the active surface area of the electrode.

Effect of inter-electrode distance (IED) in the removal of RR2

Variation in the inter-electrode distance in the electrocoagulation reactor affects the shear rate of solution, which in turn affects the average size of coagulated flocs (Spicer *et al.* 1996). The inter-electrode distance is varied from 2 to 4 cm to analyse the colour removal efficiency and charge loading on RR2 containing solution. A decrease in the colour removal efficiency was observed from 81.86 to 76.67% when the IED increased from 2 to 4 cm. The observation may be attributed to the longer migration time required for the electro generated Al (III) ions from the anode and the hydroxide ions (OH^-) from the cathode. The generated Al (III) ions are readily oxygenated and become less reactive. The generated hydrogen bubbles are not adequate to help the flotation of flocs at high electrode distance (Mbacké *et al.* 2016). The required charge loading for dye

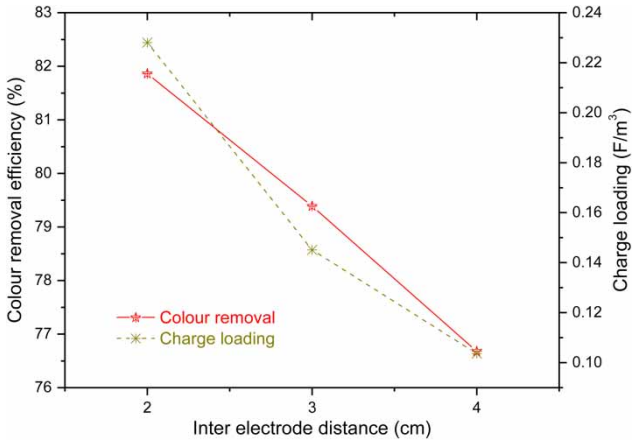

Figure 4 | Effect of inter electrode distance on the removal of RR2.

removal after 60 min of electrolysis is calculated using the following formula (Kobya *et al.* 2016):

$$Charge\ loading\left(\frac{F}{m^3}\right) = \frac{I \cdot t}{F \cdot v} \tag{15}$$

where I is electrical current (A), t is time (sec), F is Faraday's constant (96,485.33 coulombs), and v is the volume of solution obtained for the electrocoagulation process (m^3).

The charge loading decreases from 12.45 to 4.95 F/m^3 by increasing IED from 2 to 4 cm (Figure 4). The increase in electrode distance causes resistance to the passage of current into the solution. This leads to low current intensity during electrocoagulation by simultaneously reducing charge loading. The decrease in charge loading directly affects the quantity of floc generation and colour removal efficiency.

The effective removal of RR2 using Al electrodes ranges from 98 to 100%. While varying the interelectrode distance from 2 to 4 cm, this observation can be attributed to the possibility that an increase in the inter-electrode distance increases the discharge of Al ions into the solution. Similar results have been observed by Singh *et al.* (2014).

Operational cost analysis for the removal of RR2

The operational cost for electrocoagulation on the removal of RR2 from aqueous solution is calculated as:

$$OC = aENC + bELC + cCC \tag{16}$$

where OC is the operational cost ($/kg dye), ENC is the electrical energy consumption (kWh/kg dye), ELC is the electrode consumption (kg/kg dye) and CC is the chemical used (kg/kg dye) (Sakthisharmila *et al.* 2018).

The operational cost was analysed with respect to the applied voltage. The derived analysis shows that the increase in applied voltage from 2 to 6 V leads to an operational cost increase from 0.92 to 3.54 $/kg dye. The increase in applied voltage leads to more energy and electricity consumption by increasing the current density. Hence, the current density needs to be optimised before the application of the electrocoagulation at industrial scale.

UV-visible spectral studies

The UV-Vis spectra of RR2 recorded at an initial dye concentration of 300 ppm and an initial pH of 7 at frequent time intervals during the electrocoagulation process is depicted in Figure 5. Before the treatment of RR2 dye, the peaks observed at 214, 232, 282, 314 and 535 nm represent the presence of aromatic substituted benzenes, substituted naphthalene ring and $n \rightarrow \pi^*$ transition of the $N=N$ group. Further into the electrocoagulation process, the peaks at time intervals 10–60 min show a gradual decrease in intensity, no-peak shifts are also observed. These observations support the adsorption mechanism followed for the removal of RR2 using Al electrodes.

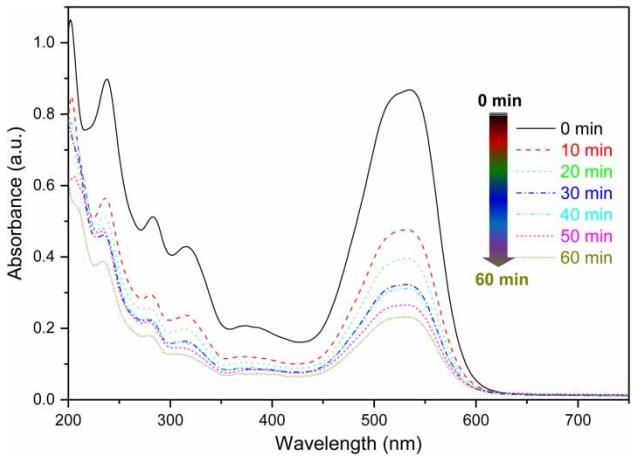

Figure 5 | UV-visible spectrum of RR2 on different time intervals during the electrocoagulation process.

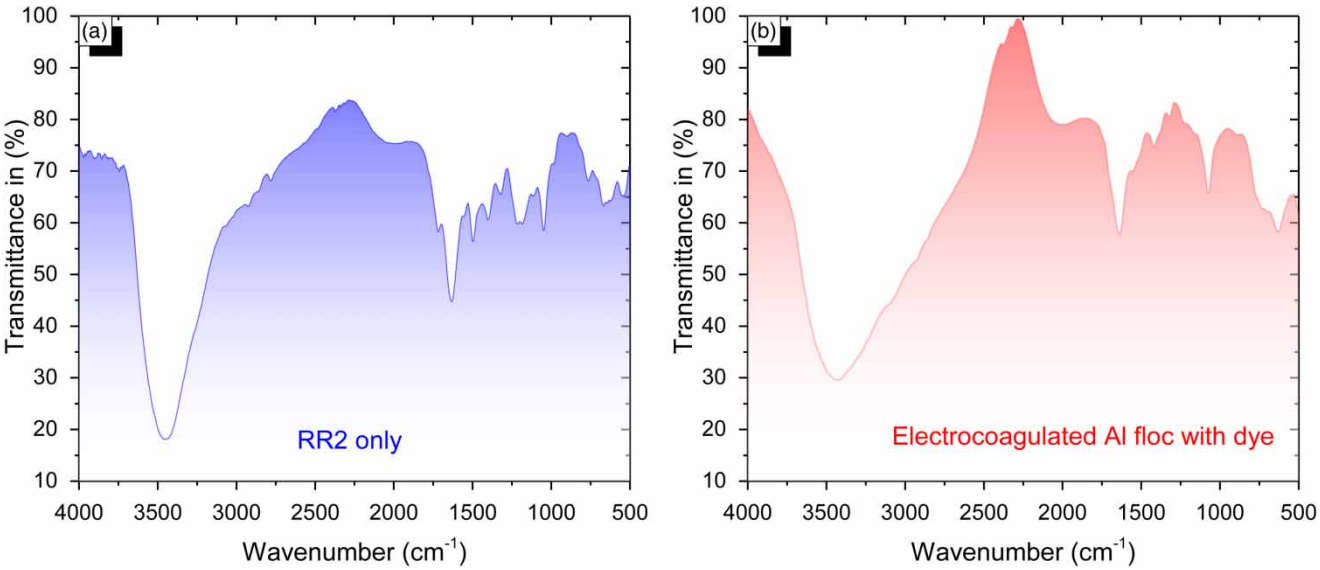

Figure 6 | FTIR spectrum of (a) RR2 dye alone and (b) electrocoagulated flocs with dye.

FTIR spectral studies of the electrocoagulated flocs

The FTIR spectra of dye before treatment (RR2 alone) and after treatment with electrocoagulated Al flocs are shown in Figure 6(a) and 6(b). The peaks at 3,452.56 and 3,428.81 cm^{-1} of the dye alone and electrocoagulated flocs with dye correspond to the existence of O-H and N-H stretching vibrations. The peak shift from 3,452 and 3,428 cm^{-1} is due to the adsorption of dye on the electrocoagulated flocs. Similarly, the peaks at 1,630.16 and 1,638.23 cm^{-1} indicate the presence of the C=O group in the dye and electrocoagulated flocs with dye molecules. The stretching peak at 1,555.14 cm^{-1} shows the presence of C = C groups, and it shifted to 1,540.99 cm^{-1} for dye containing electrocoagulated flocs. The peak of the chromophoric group ($N = N$) is observed at 1,496.93 cm^{-1} which is shifted to 1,419.81 cm^{-1} in electrocoagulated flocs with dye which showed that there is no degradation of the chromophoric group during electrocoagulation. It indicates dye adsorption on flocs. The stretching vibrations of S=O peaks are observed at 1,186.54 cm^{-1} for dye alone and electrocoagulated flocs with dye. The peaks at 1,129.39, 1,048.24, and 668.21 cm^{-1} of dye are shifted to 1,156.15, 1,072.22, and 630.60 cm^{-1} in electrocoagulated flocs with dye. The above derived points supported the adsorption mechanism for the removal of RR2 using A1 electrodes (Coates 2000).

EDX analysis of electrocoagulated flocs

The electrocoagulated flocs were collected with and without dye. The flocs were dried and used for EDX analysis. The electrocoagulated flocs without dye contain 31.06% aluminium, 62.35% oxygen, 2.77% sodium, and 3.82% chlorine while the electrocoagulated flocs with dye contain 14.04% carbon, 50.38% oxygen, and 26.28% aluminium. The presence of carbon in electrocoagulated flocs supports that the dye molecules are adsorbed on the electrocoagulated flocs. The adsorption mechanism is followed for the elimination of RR2 from aqueous solution using Al electrodes (Singh *et al.* 2014; Sakthisharmila *et al.* 2017).

CONCLUSIONS

The buffering capacity of electrocoagulated aluminium flocs maintained a pH of 9 irrespective of the initial pH. The colour removal efficiency decreased with the increase of the solution pH from acidic to alkaline medium. The increase in applied voltage led to high energy consumption and COD removal efficiency. Moreover, an increase in

electrolyte concentration resulted in slight colour removal efficiency, but electrical energy, electrode consumption, and voltage drop were found to be increased. The high concentration of dye present in the solution affects the electrocoagulation process which is supported by the decrease in the pseudo first-order kinetics rate constant. The effective surface area of the electrode has a better impact on colour removal effectiveness and the amount of dye removed per unit area of the electrode decreases. The operational cost of the electrocoagulation process is favoured at low voltages of the electrocoagulation reactor. The adsorption of dyes over the electrocoagulated flocs is supported by UV-visible studies of treated samples, FTIR, and EDX analysis of dried electrocoagulated flocs.

ACKNOWLEDGEMENTS

The authors gratefully acknowledge the collaborative research conducted among the groups, institutes and universities of authors.

SUPPLEMENTARY MATERIAL

The Supplementary Material for this paper is available at https://dx.doi.org/10.2166/aqua.2020.109.

REFERENCES

Ahmadi, M. & Ghanbari, F. 2016 Optimizing COD removal from greywater by photoelectro-persulfate process using Box-Behnken design: assessment of effluent quality and electrical energy consumption. *Environ. Sci. Pollut. Res.* **23** (19), 19,350–19,361.

Al-Kdasi, A., Idris, A., Saed, K. & Guan, C. T. 2004 Treatment of textile wastewater by advanced oxidation processes – a review. *Global Nest Int. J.* **6** (3), 222–230.

Amour, A., Merzouk, B., Leclerc, J.-P. & Lapicque, F. 2016 Removal of reactive textile dye from aqueous solutions by electrocoagulation in a continuous cell. *Desal. Water Treat.* **57** (48–49), 22,764–22,773.

APHA/AWWA/WEF 2005 *Standard Methods for the Examination of Water and Wastewater*. American Public Health Association, Washington, DC, USA.

Barrera-Díaz, C., Bernal-Martínez, L. A., Natividad, R. & Peralta-Hernández, J. M. 2012 Synergy of electrochemical/O3 process with aluminum electrodes in industrial wastewater treatment. *Ind. Eng. Chem. Res.* **51** (27), 9335–9342.

Coates, J. 2000 Interpretation of Infrared Spectra, a Practical Approach. In: *Encyclopedia of Analytical Chemistry* (R. A. Meyers, ed.). John Wiley & Sons Ltd., Chichester, pp. 10881–10882.

Costa, M., Mota, S., Nascimento, R. F. D. & Dos Santos, A. 2010 Anthraquinone-2, 6-disulfonate (AQDS) as a catalyst to enhance the reductive decolourisation of the azo dyes Reactive Red 2 and Congo Red under anaerobic conditions. *Bioresour. Technol.* **101** (1), 105–110.

Daneshvar, N., Ashassi-Sorkhabi, H. & Tizpar, A. 2003 Decolorization of orange II by electrocoagulation method. *Separ. Purif. Technol.* **31** (2), 153–162.

Daneshvar, N., Khataee, A., Ghadim, A. A. & Rasoulifard, M. 2007 Decolorization of CI Acid Yellow 23 solution by electrocoagulation process: investigation of operational parameters and evaluation of specific electrical energy consumption (SEEC). *J. Hazard. Mater.* **148** (3), 566–572.

El-Ashtoukhy, E. Z. & Amin, N. 2010 Removal of acid green dye 50 from wastewater by anodic oxidation and electrocoagulation – a comparative study. *J. Hazard. Mater.* **179** (1), 113–119.

Feng, W., Nansheng, D. & Helin, H. 2000 Degradation mechanism of azo dye CI reactive red 2 by iron powder reduction and photooxidation in aqueous solutions. *Chemosphere* **41** (8), 1233–1238.

Ghaly, A., Ananthashankar, R., Alhattab, M. & Ramakrishnan, V. 2014 Production, characterization and treatment of textile effluents: a critical review. *J. Chem. Eng. Process. Technol.* **5** (1), 1–19.

Ghosh, D., Medhi, C., Solanki, H. & Purkait, M. 2008 Decolorization of crystal violet solution by electrocoagulation. *J. Environ. Protect. Sci.* **2** (1), 25–35.

He, Z., Song, S., Qiu, J., Yao, J., Cao, X., Hu, Y. & Chen, J. 2007 Decolorization of CI Reactive Yellow 84 in aqueous solution by electrocoagulation enhanced with ozone: influence of operating conditions. *Environ. Technol.* **28** (11), 1257–1263.

Khosravi, R., Fazlzadehdavil, M., Barikbin, B. & Hossini, H. 2015 Electro-decolorization of Reactive Red 198 from aqueous solutions using aluminum electrodes systems: modeling and optimization of operating parameters. *Desal. Water Treat.* **54** (11), 3152–3160.

Kim, T.-H., Park, C., Shin, E.-B. & Kim, S. 2002 Decolorization of disperse and reactive dyes by continuous electrocoagulation process. *Desalination* **150** (2), 165–175.

Kobya, M., Demirbas, E. & Ulu, F. 2016 Evaluation of operating parameters with respect to charge loading on the removal efficiency of arsenic from potable water by electrocoagulation. *J. Environ. Chem. Eng.* **4** (2), 1484–1494.

Kuo, C.-Y. & Lin, H.-Y. 2009 Photodegration of CI Reactive Red 2 by platinized titanium dioxide. *J. Hazard. Mater.* **165** (1), 1243–1247.

Lin, C.-C. & Chen, S.-C. 2017 Decolorization of Reactive Red 2 in aqueous solutions using RPB-prepared nanoscale zero-valent iron. *Chem. Eng. Process. Process Intens.* **119**, 1–6.

Lin, C.-C., Lin, Y.-S. & Ho, J.-M. 2016 Adsorption of Reactive Red 2 from aqueous solutions using Fe_3O_4 nanoparticles prepared by co-precipitation in a rotating packed bed. *J. Alloys Compd.* **666**, 153–158.

Manikandan, P., Palanisamy, P., Baskar, R., Sivakumar, P. & Sakthisharmila, P. 2015 Physico chemical analysis of textile industrial effluents from Tirupur city, TN, India. *Int. J. Adv. Res. Sci. Eng.* **4**, 93–104.

Mbacké, M. K., Kane, C., Diallo, N. O., Diop, C. M., Chauvet, F., Comtat, M. & Tzedakis, T. 2016 Electrocoagulation process applied on pollutants treatment-experimental optimization and fundamental investigation of the crystal violet dye removal. *J. Environ. Chem. Eng.* **4** (4), 4001–4011.

Mollah, M. Y., Morkovsky, P., Gomes, J. A., Kesmez, M., Parga, J. & Cocke, D. L. 2004 Fundamentals, present and future perspectives of electrocoagulation. *J. Hazard. Mater.* **114** (1), 199–210.

Muthukumar, M., Karuppiah, M. T. & Raju, G. B. 2007 Electrochemical removal of CI Acid orange 10 from aqueous solutions. *Separ. Purif. Technol.* **55** (2), 198–205.

Nandi, B. K. & Patel, S. 2014 Removal of brilliant green from aqueous solution by electrocoagulation using aluminum electrodes: experimental, kinetics, and modeling. *Separ. Sci. Technol.* **49** (4), 601–612.

Nandi, B. K. & Patel, S. 2017 Effects of operational parameters on the removal of brilliant green dye from aqueous solutions by electrocoagulation. *Arab. J. Chem.* **10**, S2961–S2968.

Nguyen, D.-D., Kim, S.-D. & Yoon, Y.-S. 2014a Enhanced phosphorus and COD removals for retrofit of existing sewage treatment by electrocoagulation process with cylindrical aluminum electrodes. *Desal. Water Treat.* **52** (13–15), 2388–2399.

Nguyen, D. D., Ngo, H. H. & Yoon, Y. S. 2014b A new hybrid treatment system of bioreactors and electrocoagulation for superior removal of organic and nutrient pollutants from municipal wastewater. *Bioresour. Technol.* **153**, 116–125.

Nguyen, D. D., Ngo, H. H., Guo, W., Nguyen, T. T., Chang, S. W., Jang, A. & Yoon, Y. S. 2016 Can electrocoagulation process be an appropriate technology for phosphorus removal from municipal wastewater? *Sci. Total Environ* **563–564**, 549–556.

Nguyen, D. D., Yoon, Y. S., Bui, X. T., Kim, S. S., Chang, S. W., Guo, W. & Ngo, H. H. 2017 Influences of operational parameters on phosphorus removal in batch and continuous electrocoagulation process performance. *Environ. Sci. Pollut. Res.* **24** (32), 25,441–25,451.

Ozyonar, F. & Karagozoglu, B. 2011 Operating cost analysis and treatment of domestic wastewater by electrocoagulation using aluminum electrodes. *Pol. J. Environ. Stud.* **20** (1), 173–179.

Pajootan, E., Arami, M. & Mahmoodi, N. M. 2012 Binary system dye removal by electrocoagulation from synthetic and real colored wastewaters. *J. Taiwan Inst. Chem. Eng.* **43** (2), 282–290.

Pirkarami, A. & Olya, M. E. 2014 Removal of dye from industrial wastewater with an emphasis on improving economic efficiency and degradation mechanism. *J. Saudi Chem. Soc.* **21**, S179–S186.

Sakthisharmila, P., Palanisamy, P. & Manikandan, P. 2017 A characteristic study on generation and interactive effect of electrocoagulated floc with Direct Green 1 and Reactive Red 2. *J. Mol. Liq.* **231**, 160–167.

Sakthisharmila, P., Palanisamy, P. & Manikandan, P. 2018 Removal of benzidine based textile dye using different metal hydroxides generated in situ electrochemical treatment – A comparative study. *J. Clean. Prod.* **172**, 2206–2215.

Sala, M., López-Grimau, V. & Gutiérrez-Bouzán, C. 2014 Photo-electrochemical treatment of reactive dyes in wastewater and reuse of the effluent: method optimization. *Materials* **7** (11), 7349–7365.

Salmani, E. R., Ghorbanian, A., Ahmadzadeh, S., Dolatabadi, M. & Nemanifar, N. 2016 Removal of reactive red 141 dye from synthetic wastewater by electrocoagulation process: investigation of operational parameters. *Iran. J. Health Safety Environ.* **3** (1), 403–411.

Şengil, İ. A. & Özacar, M. 2009 The decolorization of CI Reactive Black 5 in aqueous solution by electrocoagulation using sacrificial iron electrodes. *J. Hazard. Mater.* **161** (2), 1369–1376.

Singh, S., Srivastava, V. C. & Mall, I. D. 2014 Electrochemical treatment of dye bearing effluent with different anode–cathode combinations: mechanistic study and sludge analysis. *Ind. Eng. Chem. Res.* **53** (26), 10,743–10,752.

Sonai, G. G., de Souza, S. M. G. U., de Oliveira, D. & de Souza, A. A. U. 2016 The application of textile sludge adsorbents for the removal of Reactive Red 2 dye. *J. Environ. Manage.* **168**, 149–156.

Spicer, P. T., Pratsinis, S. E., Trennepohl, M. D. & Meesters, G. H. 1996 Coagulation and fragmentation: the variation of shear rate and the time lag for attainment of steady state. *Ind. Eng. Chem. Res.* **35** (9), 3074–3080.

Thiyagarajan, E., Saravanan, P., Saranya, P., Gandhi, N. N. & Renganathan, S. 2013 Biosorption of reactive red 2 using positively charged Metapenaeus monoceros shells. *J. Saudi Chem. Soc.* **21**, S1–S6.

Wu, C.-H. & Ng, H.-Y. 2008 Degradation of CI Reactive Red 2 (RR2) using ozone-based systems: comparisons of decolorization efficiency and power consumption. *J. Hazard. Mater.* **152** (1), 120–127.

Wu, J., He, Z., Du, X., Zhang, C. & Fu, D. 2016 Electrochemical degradation of acid orange II dye using mixed metal oxide anode: role of supporting electrolytes. *J. Taiwan Inst. Chem. Eng.* **59**, 303–310.

Yuksel, E., Eyvaz, M. & Gurbulak, E. 2013 Electrochemical treatment of colour index reactive orange 84 and textile wastewater by using stainless steel and iron electrodes. *Environ. Progr. Sustain. Energy* **32** (1), 60–68.

First received 19 July 2019; accepted in revised form 15 November 2019. Available online 17 February 2020